Evidence for spatial variation of the fine structure constant

J. K. Webb[1], J. A. King[1], M. T. Murphy[2], V. V. Flambaum[1], R. F. Carswell[3], and M. B. Bainbridge[1]
[1]*School of Physics, University of New South Wales, Sydney, NSW 2052, Australia*
[2]*Centre for Astrophysics and Supercomputing, Swinburne University of Technology, Mail H39, PO Box 218, Victoria 3122, Australia and*
[3]*Institute of Astronomy, Madingley Road, Cambridge, CB3 0HA, England.*

(Dated: August 25, 2010)

We previously reported observations of quasar spectra from the Keck telescope suggesting a smaller value of the fine structure constant, α, at high redshift. A new sample of 153 measurements from the ESO Very Large Telescope (VLT), probing a different direction in the universe, also depends on redshift, but in the opposite sense, that is, α appears on average to be larger in the past. The combined dataset is well represented by a spatial dipole, significant at the 4.1σ level, in the direction right ascension 17.3 ± 0.6 hours, declination -61 ± 9 degrees. A detailed analysis for systematics, using observations duplicated at both telescopes, reveals none which are likely to emulate this result.

PACS numbers: 06.20.Jr, 95.30.Dr, 95.30.Sf, 98.62.Ra, 98.80.-k, 98.80.Es, 98.80.Jk

Quasar spectroscopy as a test of fundamental physics.— The vast light-travel times to distant quasars allows us to probe physics at high redshift. The relative positions of wavenumbers, ω_z, of atomic transitions detected at redshift $z = \lambda_{obs}/\lambda_{lab} - 1$, can be compared with laboratory values, ω_0, via the relationship $\omega_z = \omega_0 + Q\left(\alpha_z^2 - \alpha_0^2\right)/\alpha_0^2$ and the coefficient Q measures the sensitivity of a given transition to a change in α. The variation in both magnitude and sign of Q for different transitions is a significant advantage of the Many Multiplet method [1, 2], helping to combat potential systematics.

The first application of this method, 30 measurements of $\Delta\alpha/\alpha = (\alpha_z - \alpha_0)/\alpha_0$, signalled a smaller α at high redshift at the 3σ significance level. By 2004 we had made 143 measurements of α covering a wide redshift range, using further data from the Keck telescope obtained by 3 separate groups, supporting our earlier findings, that towards that general direction in the universe at least, α may have been smaller at high redshift, at the 5σ level [3–5]. The constant factor at that point was (undesirably) the telescope/instrument.

Subsequently, only 1 further independent statistical study has been completed [6], but difficulties with the analysis methods mean those results do not add to or provide a check on our earlier results [7]. A small number of individual α measurements have been made, but provide no general conclusions since the systematic component of the error on $\Delta\alpha/\alpha \sim 10^{-5}$.

New data from the VLT.— We have now analysed a large dataset from a different observatory, the VLT. Full details and searches for systematic errors will be given elsewhere[8, 9]. Here we summarize the evidence for spatial variation in α emerging from the combined Keck+VLT samples. Quasar spectra, obtained from the ESO Science Archive, were selected, prioritising primarily by expected signal to noise but with some preference given to higher redshift objects and to objects giving more extensive sky coverage. The ESO MIDAS pipeline was used for the first data reduction step, including wavelength calibration, although enhancements were made to derive a more robust and accurate wavelength solution from an improved selection of thorium-argon calibration lamp emission lines [10]. Echelle spectral orders from several exposures of a given quasar were combined using UVES_POPLER [11]. A total of 60 quasar spectra from the VLT have been used for the present work, yielding 153 absorption systems. Absorption systems were identified via a careful visual search of each spectrum, using RDGEN [12], scanning for commonly detected transitions at the same redshift, hence aligned in velocity coordinates. Several transition matches were required for acceptance and, given the high spectral resolution, chance matches were eliminated.

Absorption system modelling.— As in our previous studies, VPFIT was used to model the profiles in each absorption system [13] with some enhancements, described in [8]. A comprehensive list of the transitions used, their laboratory wavelengths, oscillator strengths, and Q coefficients are compiled in [4, 8].

The following general procedures were adhered to: *(i)* For each absorption system, physically related parameters (redshifts and b-parameters) are tied, in order to minimise the required number of free parameters and derive the strongest possible constraints on line positions, and hence $\Delta\alpha/\alpha$. *(ii)* Parameters were tied only for species with similar ionisation potentials, to minimise possible introduction of random effects on α, mimicked by spatial (and hence velocity) segregation effects; *(iii)* Line broadening is typically dominated by turbulent rather than thermal motion. Both limiting-case models were applied and $\Delta\alpha/\alpha$ determined for each. The final $\Delta\alpha/\alpha$ was derived from a likelihood-weighted average. Details and justification are given in [8]; *(iv)* Where appropriate (and where available), isotopic structures are included in the fitting procedure (for MgI, MgII, AlIII, SiII, and FeII); *(v)* Velocity structures were determined initially choosing the strongest unsaturated transitions in each system. Normalised residuals across each transition fitted were examined and the fit progressively refined with the introduction of each additional transition to the fit; *(vi)* Transitions falling in spectral regions contaminated by telluric features or atmospheric absorption were discarded. Any data regions contaminated by cosmic rays, faulty CCD pixels, or any other unidentified noise effects, were also discarded; *(vii)* A few gravitational lenses were identified by being difficult or impossible to model successfuly. The non-point source quasar image and the resultant complex line-of-sight geometry can significantly alter apparent relative line strengths. These systems were discarded; *(viii)* In all cases we derived the final model without solving for $\Delta\alpha/\alpha$. The introduction of $\Delta\alpha/\alpha$ as an additional free parameter was only done once the profile velocity structure had been finalised, eliminating any possible bias towards a 'preferred' $\Delta\alpha/\alpha$. One potential consequence of this approach might conceivably be a small bias on $\Delta\alpha/\alpha$ *towards* zero, should some 'fitting-away' of $\Delta\alpha/\alpha$ occur, by column density adjustments or velocity structure decisions. The reverse is not true, i.e. it cannot bias towards a non-zero $\Delta\alpha/\alpha$.

VPFIT [13] minimises χ^2 simultaneously over all species. Whilst the strongest components may appear in all species, weaker components can sometimes fall below the detection threshold and hence are excluded, such that a component which appears in MgII, for example, does not appear in FeII. There is no solution to this (known) problem but its effect merely adds an additional random scatter on $\Delta\alpha/\alpha$ for an ensemble of observations.

Spatially dependent α.— An initial inspection of $\Delta\alpha/\alpha$ vs redshift for the new VLT dataset reveals a redshift trend, opposite in sign compared to the earlier Keck data. Splitting each sample at $z = 1.8$, our 2004 Keck sample [5] gave $\langle\Delta\alpha/\alpha\rangle_{z<1.8} = -0.54 \pm 0.12 \times 10^{-5}$ and $\langle\Delta\alpha/\alpha\rangle_{z>1.8} = -0.74 \pm 0.17 \times 10^{-5}$. The present 2010 VLT sample, which will be discussed in detail in [8] gives $\langle\Delta\alpha/\alpha\rangle_{z<1.8} = -0.06 \pm 0.16 \times 10^{-5}$ and $\langle\Delta\alpha/\alpha\rangle_{z>1.8} = +0.61 \pm 0.20 \times 10^{-5}$. Errors here and throughout this paper are 1σ estimates.

Errors on individual $\Delta\alpha/\alpha$ values for the VLT sample are $\sigma^2_{tot} = \sigma^2_{stat} + \sigma^2_{sys}$, where σ^2_{sys} was derived empirically using a modification of the Least Trimmed Squares (LTS) method, where only 85% of data, those points with the smallest squared residuals, are fitted. σ_{sys} was assumed constant for all VLT absorbers and was found to be $\approx 0.88 \times 10^{-5}$, showing that the scatter in the VLT $\Delta\alpha/\alpha$ is greater than expected on the basis of statistical-errors alone. Errors on $\Delta\alpha/\alpha$ for the Keck sample are discussed in [4], although we derive a new estimate of σ_{sys} for the Keck points using the LTS method.

The Keck (Mauna Kea, Hawaii) and VLT (Paranal, Chile) locations on Earth are separated by 45° in latitude and hence, on average, observe different directions on the sky. We are thus motivated to explore a simple spatial dependence using the combined dataset.

The Keck sample we use is as presented in [5] with a minor modification: 3 points were removed. 2 had been included erroneously (from a spectrum known to have calibration problems) and 1 further point was clipped, having a residual greater than 3σ against a modified LTS fit to the Keck data.

Initially the 3 datasets (i.e. Keck, VLT and combined) are fitted using a simple possible dipole+monopole model, represented here by $\Delta\alpha/\alpha = A\cos\Theta + m$, where m is a constant allowing an offset from the terrestrial value, Θ is the angle on the sky between quasar sightline and best-fit dipole position, and A is the dipole amplitude.

To examine the probability of the observed dipole model arising by chance, we bootstrap the sample, repeatedly randomising the association between $\Delta\alpha/\alpha$ and quasar sightline, fitting $\Delta\alpha/\alpha = A\cos\Theta + m$ at each realisation. We then numerically determine the probability of obtaining a value of χ^2 less than or equal to the actual value by comparing with the χ^2 probability distribution from the bootstrap process.

Figure 1 illustrates the best-fit dipole equatorial coordinates on an all-sky map, with approximate 1σ error contours derived from the covariance matrix. Figure 2 illustrates the $\Delta\alpha/\alpha$ binned data and the best-fit dipole model. Best-fit parameters are given in the captions.

As a second trial model, allowing for a spatial gradient in α, we assign a distance to each $\Delta\alpha/\alpha$ measurement of $r(z) = ct(z)$ where c is the speed of light and $t(z)$ is the look-back time at redshift z. The model is then $\Delta\alpha/\alpha = Br(z)\cos\Theta + m$. Figure 3 illustrates $\Delta\alpha/\alpha$ vs look-back time distance projected onto the dipole axis, $r\cos\Theta$, using the best-fit dipole parameters for this model. This model seems to represent the data reasonably well and the data show a strong correlation, significant at the 4.1σ level.

Given the relatively low statistical significance of the monopole term m for both models above (see captions, Figures 2 and 3), and because the theoretical interpretation of a monopole term is unclear, a third model was fitted, $\Delta\alpha/\alpha = Br\cos\Theta$, giving $B = 1.10 \pm 0.25 \times 10^{-6}$ GLyr^{-1} with a significance of 4.2σ and giving parameters right ascension 17.4 ± 0.6 hours, declination -58 ± 6 degrees.

An alternative to empirically increasing the $\Delta\alpha/\alpha$ error bars to incorporate a systematic component is to assume $\sigma^2_{tot} = \sigma^2_{stat}$ and to iteratively trim the data during model fitting. This provides a further stringent test of whether the apparent gradient in α is dominated by a subset of the data, perhaps more prone to some unknown systematic than the remainder. Adopting $\sigma^2_{tot} = \sigma^2_{stat}$ will clearly result in higher significance levels. In Figure 4 we plot the statistical significance of the dipole in units of σ and find that over 40% of the data must be discarded

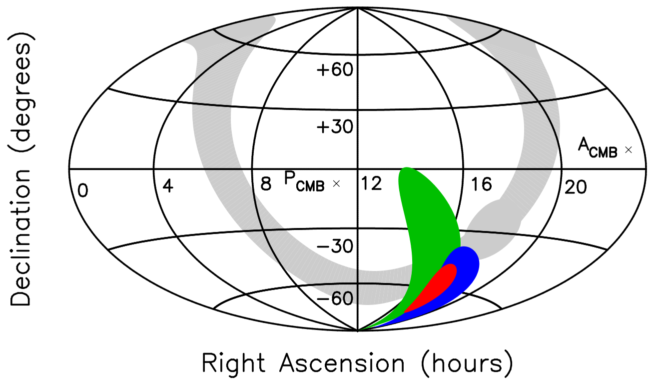

FIG. 1. All-sky plot showing the independent Keck (green) and VLT (blue) best-fit dipoles, and the combined sample (red), in equatorial co-ordinates. Approximate 1σ confidence contours are from the covariance matrix. A bootstrap analysis gives the chance-probability of getting the observed (or better) alignment between the independent Keck and VLT dipoles is only 4%. The cosmic microwave background dipole and antipole are illustrated for comparison.

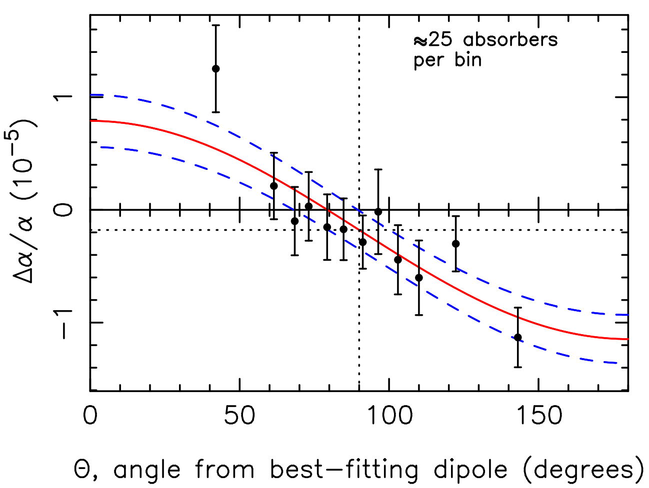

FIG. 2. $\Delta\alpha/\alpha$ for the combined Keck and VLT data vs angle Θ from best-fit dipole, $\Delta\alpha/\alpha = A\cos\Theta + m$, $A = (0.97 \pm 0.21) \times 10^{-5}$ and $m = (-0.18 \pm 0.08) \times 10^{-5}$. Dashed lines illustrate $\pm1\sigma$ errors on the dipole fit. The best-fit dipole is at right ascension 17.3 ± 0.6 hours, declination -61 ± 9 degrees and is statistically preferred over a monopole model at the 4.1σ level.

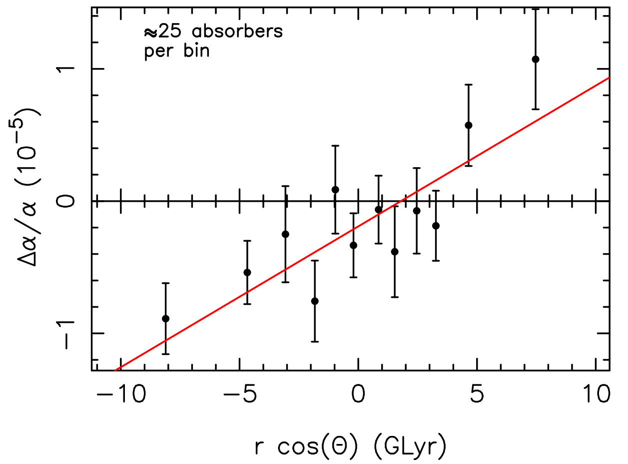

FIG. 3. $\Delta\alpha/\alpha$ vs $Br\cos\Theta$ for the model $\Delta\alpha/\alpha = Br\cos\Theta + m$ showing the gradient in α along the best-fit dipole. The best-fit direction is at right ascension 17.4 ± 0.6 hours, declination -62 ± 6 degrees, for which $B = (1.1 \pm 0.2) \times 10^{-6}$ GLyr^{-1} and $m = (-1.9 \pm 0.8) \times 10^{-6}$. This dipole+monopole model is statistically preferred over a monopole-only model also at the 4.1σ level. A cosmology with parameters $(H_0, \Omega_M, \Omega_\Lambda) = (70.5, 0.2736, 0.726)$ was used [14].

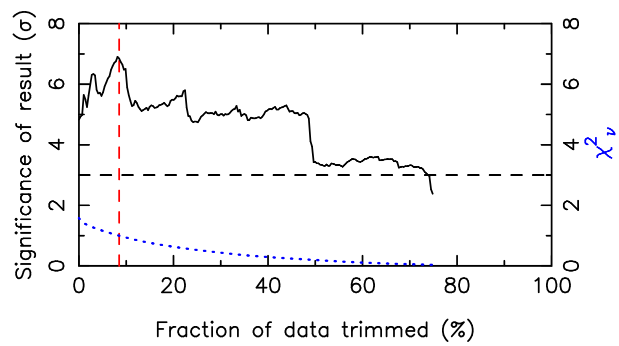

FIG. 4. As an alternative to increasing $\Delta\alpha/\alpha$ error bars, to account for the additional scatter in the data as described in the text, we instead use $\sigma_{tot}^2 = \sigma_{stat}^2$ and iteratively clip the most deviant $\Delta\alpha/\alpha$ value, fitting $\Delta\alpha/\alpha = A\cos\Theta + m$. The vertical dashed line illustrates where the dotted curve $\chi_\nu^2 = 1$, when $\sim 8\%$ of the data has been trimmed. Almost 50% of the data must be discarded before the significance drops below 4σ showing that the dipole signal is generally present in entire dataset.

to push the result below 4σ, implying a remarkable internal consistency within the data.

Empirical test for systematics.— One potential effective relative distortion might be due to slight mechanical mis-alignments of the spectrograph slits for the 2 arms, red and blue, of the UVES spectrograph on the VLT. However, this specific effect appears to be substantially smaller than required to explain values of $\Delta\alpha/\alpha \sim 10^{-5}$ seen in the present work [15].

A more subtle but related effect may be slight off-centre placement of the quasar image in the spectrograph slit, by different amounts for different exposures, at different wavelength settings. This may apply to either or both Keck and VLT spectra. Since spectrograph slit illuminations are different for quasar (point source) and ThAr calibration lamp (uniform illumination), the subsequent combination of individual exposures to form a 1-dimensional spectrum may then contain relative velocity shifts between spectral segments coming from different exposures. This effect will exist in our data at some level and it is clearly important to know the impact on an ensemble of measurements of α.

Fortunately, 6 quasars in our sample have both Keck and VLT spectra, allowing a direct and empirical check on the effect above, and indeed any other systematics which produce relative velocity shifts along the spectrum. To do this we selected small spectral segments, each a few Å wide, flanked by unabsorbed continuum flux from the quasar, and fitted Voigt profiles using VPFIT, but adding an additional free parameter allowing a velocity shift between the Keck and VLT segments, $\delta v(\lambda_{obs})_i$, where λ_{obs} is the observed wavelength and i refers to the i^{th} quasar. All available absorption lines in the 6 spectra were used, including both Lyman-α forest lines and heavy element lines but excluding telluric features. In this way we can map any effective relative distortions in the calibrations between each pair of spectra. A total of 694 measurements were used from the 6 pairs of spectra over the observed wavelength range $3506 < \lambda < 8945$Å.

We formed a composite function $\delta v(\lambda_{obs})$ after first normalising $\langle \delta v(\lambda_{obs})_i \rangle = 0$ for each i to remove any potential small constant velocity offsets from each spectrum (expected from off-centering of the quasar in the spectrograph slit), which cannot influence α.

Finally we fit the composite $\delta v_{\lambda_{obs}}$ with a linear function $f(\delta v) = a\lambda_{obs} + b$ where $a = (-7 \pm 14) \times 10^{-5}\,\mathrm{km\,s^{-1}\,Å^{-1}}$, $b = 0.38 \pm 0.71\,\mathrm{km\,s^{-1}}$. The final $f(\delta v)$ thus shows a weak (but statistically insignificant) velocity drift, and provides an empirical transformation between the Keck and VLT wavelength scales. For each quasar absorption system, we modify the input laboratory wavelengths used in the Voigt profile fitting procedure λ_{lab} to $\lambda'_{lab} = \lambda_{lab} + \Delta\lambda_{lab}$ where $\Delta\lambda_{lab} = \lambda_{lab}\,\delta v\,(\lambda_{obs})/c$, and finally use the λ'_{lab} to re-compute $\Delta\alpha/\alpha$ for the entire sample. Since we do not know whether the Keck or the VLT observation causes the non-zero values of the parameters a, b above, we applied the transformation separately to both and examine the impact in each case.

There was one complicating aspect of this effect excluded from the discussion above, arising from a 7^{th} spectral pair. The $\delta v(\lambda_{obs})_7$ showed a more significant non-zero slope than the other 6, suggesting a small but significant calibration problem with that particular spectrum. We therefore applied a slightly more complicated transformation to the data to allow for this, using a Monte Carlo simulation to estimate the potential impact on our full combined Keck and VLT sample of both the previous effect measured in 6 quasars *plus* the effect derived from the 7^{th} quasar simultaneously, applied in appropriate proportions. The full details of this analysis will be discussed separately in [9].

A systematic of the same magnitude as that from the 7^{th} pair cannot be present in any large fraction of our data, otherwise it would generate large numbers of noticeable outliers. If we apply $f(\delta v)$ from the 6 quasar pairs, the significance of the dipole is reduced to 3.1σ. Blindly including the effect of the 7^{th} pair under a Monte Carlo method reduces the significance to a most likely value of 2.2σ. However, in this circumstance we add significant amounts of extra scatter into the data above what is already observed, implying that this is an overestimate of a systematic effect of this type. Additionally, the trend of $\delta v(\lambda_{obs})_i$ against wavelength is different in magnitude and sign for each quasar pair, implying that these effects are likely to average out for an ensemble of observations. Thus, application of the effect as described above should be regarded as extreme in terms of impact on estimating $\Delta\alpha/\alpha$.

Conclusions.— Quasar spectra obtained using 2 separate observatories reveal a spatial dependence of the fine stucture constant at a significance of 4.1σ, estimated conservatively, taking into account both statistical and systematic errors. Two independent datasets reveal a striking internal consistency and the directions of the independently derived spatial dipoles agree well, with a chance probability of 4%. The apparent symmetry in magnitude of the $\Delta\alpha/\alpha$ variation between northern and southern hemisphere quasar data is also striking. A subset of the quasar spectra observed at both observatories permits a direct test for systematics. None are found which are likely to emulate the apparent cosmological dipole in α we detect. To explain our results in terms of systematics will require at least 2 different and finely tuned effects. Future similar measurements targeting the apparent pole and anti-pole directions will maximise detection sensitivity, and further observations duplicated on 2 independent telescopes will better constrain systematics. Above all, an independent technique is required to check these results. Qualitatively, our results suggest a violation of the Einstein Equivalence Principle, and could infer a very large or infinite universe, within which our 'local' Hubble volume represents a tiny fraction, with correspondingly small variations in the physical constants.

This work is supported by the Australian Research Council. RFC is grateful to the Leverhulme Trust for an Emeritus grant. We thank Steve Curran, Elliott Koch, Julian Berengut, John Barrow and Paul Davies for discussions throughout this work.

[1] J. K. Webb *et al.*, Phys. Rev. Lett. **82**, 884 (Feb. 1999), arXiv:astro-ph/9803165.
[2] V. A. Dzuba, V. V. Flambaum, and J. K. Webb, Phys. Rev. Lett. **82**, 888 (Feb. 1999), arXiv:physics/9802029.
[3] J. K. Webb *et al.*, Phys. Rev. Lett. **87**, 091301 (Aug. 2001), arXiv:astro-ph/0012539.
[4] M. T. Murphy, J. K. Webb, and V. V. Flambaum, Mon. Not. Roy. Astron. Soc. **345**, 609 (Oct. 2003), arXiv:astro-ph/0306483.
[5] M. T. Murphy, V. V. Flambaum, and J. K. Webb, in *Astrophysics, Clocks and Fundamental Constants*, Lecture Notes in Physics, Berlin Springer Verlag, Vol. 648, edited by S. G. Karshenboim & E. Peik (2004) pp. 131–150, arXiv:astro-ph/0310318.

[6] H. Chand *et al.*, Astron. Astrophys. **417**, 853 (Apr. 2004), arXiv:astro-ph/0401094.
[7] M. T. Murphy, J. K. Webb, and V. V. Flambaum, Mon. Not. Roy. Astron. Soc. **384**, 1053 (Mar. 2008), arXiv:astro-ph/0612407.
[8] J. A. King *et al.*(2010), in preparation; to be submitted to Mon. Not. Roy. Astron. Soc.
[9] F. E. Koch *et al.*(2010), in preparation; to be submitted to Mon. Not. Roy. Astron. Soc.
[10] M. T. Murphy *et al.*, Mon. Not. Roy. Astron. Soc. **378**, 221 (Jun. 2007), arXiv:astro-ph/0703623.
[11] M. T. Murphy, "UVES_POPLER," (2010), `http://astronomy.swin.edu.au/~mmurphy/UVES_popler`.
[12] R. F. Carswell, "RDGEN," (2004), `http://www.ast.cam.ac.uk/~rfc/rdgen.html`.
[13] R. F. Carswell and J. K. Webb, "VPFIT - Voigt profile fitting program. Version 9.5," (2010), `http://www.ast.cam.ac.uk/~rfc/vpfit.html`.
[14] G. Hinshaw *et al.*, Astrophys. J. Supp. **180**, 225 (Feb. 2009), arXiv:0803.0732.
[15] P. Molaro *et al.*, Astron. Astrophys. **481**, 559 (Apr. 2008), arXiv:0712.3345.

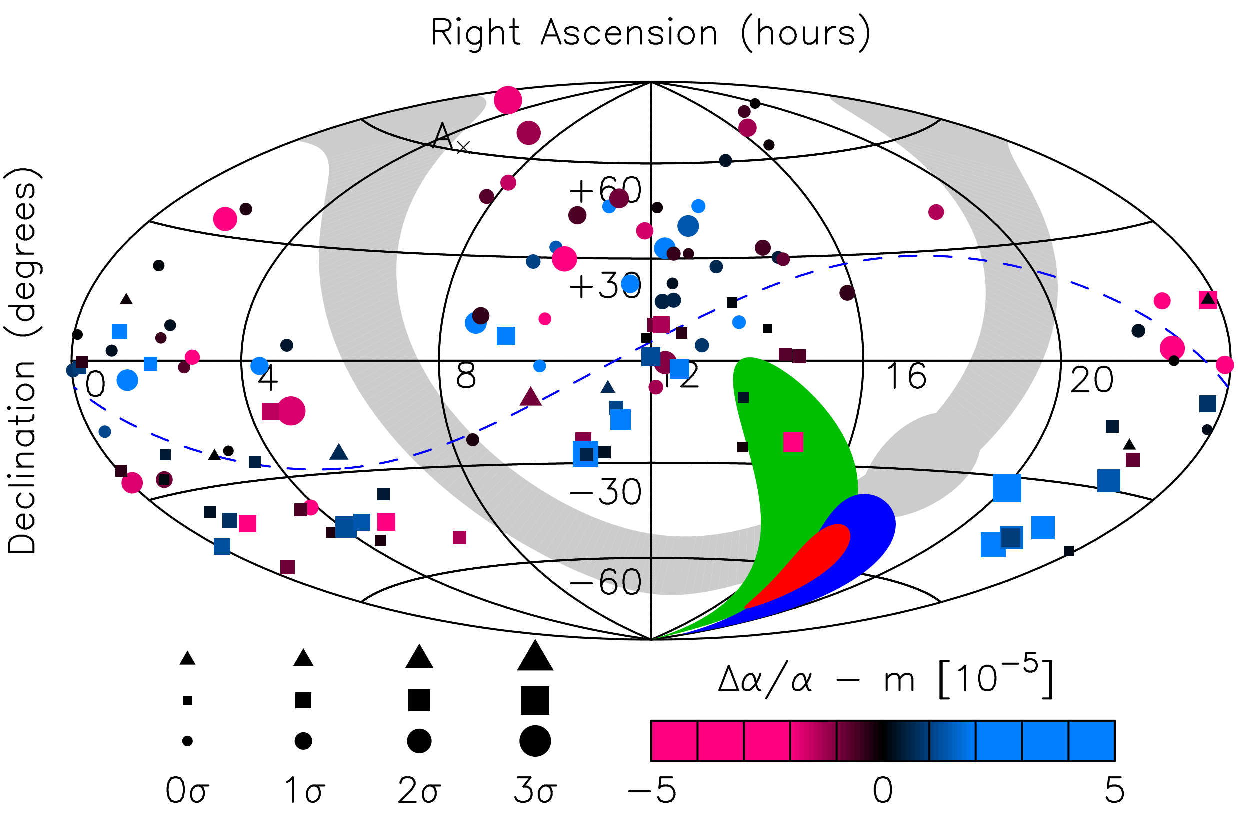

FIG. 5. Supplementary figure. All-sky illustration of the combined Keck and VLT $\Delta\alpha/\alpha$ measurements. Squares are VLT points. Circles are Keck points. Triangles are quasars observed at both Keck and VLT. Symbol size indicates deviation of $\Delta\alpha/\alpha$ from the monopole value m in $\Delta\alpha/\alpha = A\cos\Theta + m$ (Figures 2 and 3). The grey shaded area represents the Galactic plane with the Galactic centre indicated as a bulge. The blue dashed line shows the equatorial region of the α-dipole. More and larger blue squares are seen south of the equatorial region and more and larger red circles are seen north of it.